J. SE Asian Appl. Geol., Sep–Dec 2010, Vol. 2(3), pp. 185–194

A GEOTECHNICAL-HYDROLOGICAL APPROACH FOR DEFINING CRITICAL RAINFALL-INDUCED SHALLOW LANDSLIDES AND WARNING SYSTEM AT LARGE SCALE

Apip*[1], Takara, K.[2], Yamashiki, Y.[2], Ibrahim, A.B.[3], and Sassa, K.[4]

[1]*Department of Urban and Environmental Engineering, Kyoto University (Kyoto 615-8540, Japan)*
[2]*DPRI, Kyoto University (Uji 611-0011, Japan)*
[3]*Research Centre for Water Resources, Department of Public Works (Bandung 40135, Indonesia)*
[4]*International Consortium on Landslides (Kyoto 606-8226, Japan)*

Abstract

This study proposes a novel method that combines deterministic slope stability model and hydrological approach for predicting critical rainfall-induced shallow landslides. The method first uses the slope stability model to identify "where" slope instability will occur potentially; the catchment is characterized into stability classes according to critical soil saturation index. The critical saturated soil index is calculated from local topographic components and soil attributes. Then, spatial distribution of critical rainfall is determined based on a hydrological approach under near-steady state condition as a function of local critical saturated soil depth, slope geometric, and upstream contributing drainage areas. The critical rainfall mapping is bounded by theoretically "always stable" and "always unstable" areas. To show how the method works, observed landslides (1985-2008) and a satellite-based rainfall estimates associated with a past new shallow landslide in the Upper Citarum River catchment (Indonesia) were used to validate the model. The proposed study is useful for rainfall triggered shallow landslide disaster warning at large catchment scale.

Keywords: *Critical rainfall, slope stability, hydrology, shallow landslide, Citarum River catchment*.

*Corresponding author: APIP, Department of Urban and Environmental Engineering, Kyoto University (Kyoto 615-8540, Japan): apip@flood.dpri.kyoto-u.ac.jp

1 Introduction

It is well known that many shallow landslides are triggered by rainfall when shear strength is reduced because of an increase in pore-water pressure. The literature has so far suggested three general approaches for relating rainfall, soil saturation, and landslide research. First, the methods have attempted to analyze landslide triggering rainfall threshold by using historical data (Cardinali *et al.*, 2006). Second, rainfall has been used as a dynamic variable along with the static variables of land surface factors in logistic regression approaches (multivariate analysis) for landslide modeling (Dai & Lee, 2003). Third, process-based geotechnical-hydrological models is used by utilizing rainfall data as an input (Bathurst *et al.*, 2006). This last approach has appeared to capture the influence of rainfall recharge on subsurface hydrological behavior and soil mechanics in triggering shallow landslides.

Regardless of the approach, the scarcity of rain gauges has been a common problem of using rainfall for shallow landslide prediction and warning, especially in mountainous areas. For example, The Upper Citarum River catchment (2,310 km^2), as one of the persistently active landslides occurring in Indonesia is covered only by one rain gauge installed to be operated in real-time base with high time res-

olution. According to the National Agency for Meteorology and Geophysics (BMG) of Indonesia, many rain gauge locations report only daily amount, which has significant delay for flood and landslide warning system. Recent advances in satellite-based precipitation observation technology and increasing availability of its product in high resolution is providing an opportunity to deliver an alternative to rain gauges in sparsely gauged areas and ungauged.

Previous researchers have worked with satellite-based rainfall data to identify landslide potential in response to a heavy rainfall event at large and global scales (Hong & Adler, 2008). The difference between the critical rainfall threshold and estimated radar/satellite imagery-based rainfall intensity has been used for computing shallow landslide occurrence probabilities (Chiang & Chang, 2009). Therefore, this study focuses on the derivation of critical rainfall model and to evaluate its efficiency for shallow landsliding prediction and warning in mountainous areas of large catchment scale by using satellite-based rainfall data.

A geotechnical-hydrological approach is the third approach as mentioned above. It has been concentrated on deriving critical rainfall-induced shallow landslides. The approach combines an infinite slope stability model with a steady-state hydrologic approach. The method first uses the slope stability model to identify "where" potential slope instability areas, in which the catchment is characterized into stability classes according to critical soil saturation through inversion of the standard of factor of safety analysis; it is an index used to determine the slope stability. Thus, spatial distribution of the critical rainfall is determined as function of local critical saturated soil depth and upstream contributing areas. The critical rainfall mapping is bounded by theoretically "always stable" and "always unstable" areas. To demonstrate the effectiveness of this method, laboratory test of soil properties, inventory landslides, and a satellite-based rainfall estimates associated with a past new shallow landslide in the Upper Citarum catchment, Indonesia were conducted to validate the model.

The innovative aspect of the method is that the produced critical rainfall rate (mm hr^{-1}), which is the minimum steady-state rainfall predicted to cause instability, has higher temporal resolution than the current existing critical rainfall model (mm day^{-1}) (Montgomery & Dietrich, 1994). In combination with global near real-time satellite-based rainfall estimates and global topographic-hydrographic datasets, it is possible to expand the method for rainfall-triggered shallow landslide disaster preparedness and mitigation across the large catchment areas.

2 Geotechnical-hydrological model

2.1 Infinite slope stability model

Slope stability model is developed by the concept of infinite slope model, using factor of safety (FS) considering a failure surface. It assumes: (i) failure is the result of translation sliding, (ii) the failure plane and water table is parallel to the ground surface, (iii) failure occurs as a single layer, (iv) the failure plane is of infinite length, and (v) the impact of adjacent factors are not accounted. For hillslopes, the safety factor generally is represented as the ratio of the available resisting force (shear strength) to the driving force (shear stress). Instability occurs when the shear strength of a soil layer becomes smaller than the shear stress acting on the soil. The governing equation of safety factor used in this study is based on a Mohr-Coulomb failure law.

Figure 1 illustrates the forces acting on a point along the potential failure slope. The resisting force of a soil layer is the shear strength (s) as a combination of forces, including the normal stress (σ), pore pressure (μ) within the soil material, total cohesion factors (c), and the effective angle of internal friction in degree (φ). The resultant force between normal stress and pore pressure is the effective normal stress. Shear strength formulation based upon the Mohr-Coulomb law as:

$$s = c + (\sigma - \mu) \tan \phi \qquad (1)$$

 © 2010 Department of Geological Engineering, Gadjah Mada University

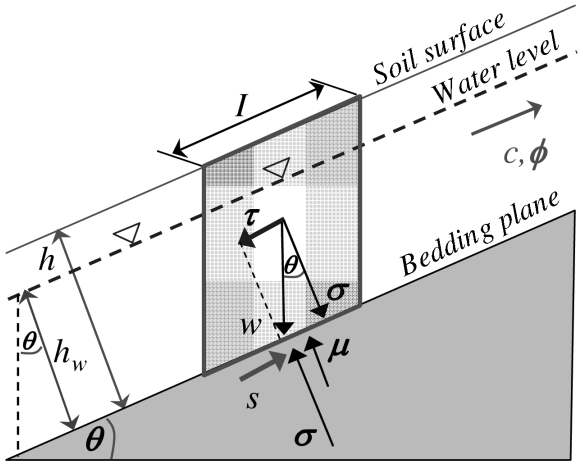

Figure 1: Forces diagram on a slice of an infinite slope.

Normal stress is the vertical component of gravity which resisting downslope movement:

$$\sigma = \rho_s \, g \, h \, \cos\theta \tag{2}$$

where ρ_s is the soil density (kg/m^3), the g is the gravitational acceleration (m/sec^2), h is the vertical soil depth (m), and θ is the slope angle (deg). Soil moisture increases the unit weight of soil material, therefore it increases both the resisting and driving forces. Soil moisture creates pore pressure, which reduces the effective normal stress and shear strength. Pore pressure is quantified by the following equation when assuming no excess pore water pressure:

$$\mu = \rho_w \, g \, h_w \, \cos\theta \tag{3}$$

where ρs is the density of water (kg/m^3) and h_w is the vertical height of the saturated depth (m). Pore pressures in the slope are different in sites and also very much varies with time. It is difficult to estimate those values and include it in this model applying for large area. Therefore, we simplified the condition of pore pressure in the slope by assuming that the pore pressure in the slope is always in the static condition, namely. This assumption gives smaller pore water pressure in the process of the saturated depth rise and greater pore water pressure in the descending process of the saturated level. In the unsaturated soil layer, suction (negative pore water pressure) is working and providing additional shear strength. This is also difficult to include in this model at present. We excluded the slope areas from the target of this research. Those slopes may fail due to the increase of moisture.

The shear stress as driving force is defined downslope parallel component of gravity as follows:

$$\tau = \rho_s \, g \, h \, \sin\theta \tag{4}$$

by substituting the formula for shear strength and shear stress, the factor of safety without considering root cohesion and vegetative surcharge equals:

$$FS = \frac{c + \cos\theta \, [1 - r_u] \, \tan\phi}{\sin\theta} \tag{5}$$

$$c = \frac{c_s}{\rho_s \, g \, h}; \; r_u = \frac{h_w \rho_w}{h \rho_s}$$

in which c_s is the soil cohesion (Pa). The dimensionless form of the Eq. (5) has been widely used to analyze the stability of shallow soil using Digital Terrain Models (Montgomery & Dietrich, 1994).

According to Eq. (5), most of the variable could be set up spatially-distributed but it is assumed that only hw is time-varying. The saturated depth hw is determined by the flux of subsurface water flow computed by hydrological model (see Eq. 1). Here the ratio ($m = h_w/h$) shows the relative saturated depth is time-dependent (between 0 and 1). Whenever FS < 1, the driving forces prevail and the potential for failure is high. Through an inversion of the standard factor of safety, a fixed time-invariant critical relative soil saturation (m^c) triggering slope failure (i.e. relative soil saturation that yields FS = 1) for each grid element could be approximated as:

$$m^c = \frac{\rho_s}{\rho_w} \left(1 - \frac{\tan\theta}{\tan\phi}\right) + \frac{c_s}{h \, \rho_w \, g \, \cos\theta \tan\phi} \tag{6}$$

Based on the concept of critical relative soil saturation, three slope stability classes could be defined: theoretically always stable, potentially stable/unstable, and theoretically always unstable. The condition for theoretically **"always**

stable" is addressed for those slopes that are stable even when saturated depth reaches the ground surface $m^c > 1$. The slopes are predicted theoretically always stable in the following equation:

$$\tan\theta < \tan\phi\left(1 - \frac{\rho_w}{\rho_s}\right) + \frac{c_s}{h\,\rho_s\,g\,\cos\theta} \qquad (7)$$

Similarly, the slopes that are predicted to be unstable even when dry condition (i.e. $m = 0$) are considered to be theoretically "always unstable". Such slopes are where suction is working or they are rocks (c, ϕ is much higher than those measured in Table 1). The condition for this slope stability class is expressed as:

$$\tan\theta \geq \tan\phi + \frac{c_s}{h\,\rho_s\,g\,\cos\theta} \qquad (8)$$

The slope elements are classified into potentially "stable/unstable" are those areas between the criteria of Eqs.(7) and (8). The critical relative soil saturation depth by using Eq.(6) and time-dependent slope instability analysis are calculated only for those grids with the slope stability classified into potentially stable/unstable.

2.2 Hydrological model

Spatial lumping of a distributed kinematic wave rainfall-runoff model, considering three lateral flow mechanisms, including (1) subsurface flow through capillary pore, (2) subsurface flow through non-capillary pore and (3) surface flow on the soil layer that was developed by authors (Apip *et al.*, 2008) is used for hydrological approach in derivating critical rainfall-induced shallow landslides. The fundamental assumption of the lumping method is that the rainfall-runoff process of the catchment system reaches a steady state with spatially uniform rainfall input. From this assumption, discharge flux can be expressed as the product of rainfall intensity and the upslope contributing areas.

From the steady state assumption, the flux of water discharge per unit width in each grid cell as shown by Figure 2 can be given as follow:

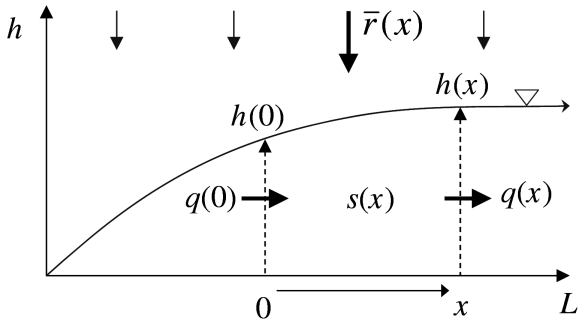

Figure 2: Schematic diagram of the kinetic wave flow model for a series of grids.

$$q(x) = q(0)/w + \bar{r}\int_0^x (x)\,dx = \bar{r}\,U/w + \bar{r}\,x \qquad (9)$$

where r is the rainfall intensity, U is the upslope contributing area, x is the horizontal distance (slope length) from the upstream end of a grid cell, and w is the width of the grid cell.

From stage-discharge relationships (Tachikawa *et al.*, 2004), a general kinematic wave equation can be expressed as $q = g(h)$:

$$q = \begin{cases} v_m d_m (h_w / d_m)^{\beta}, & o \leq h_w \leq d_m \\ v_m d_m + v_a (h_w - d_m), & d_m \leq h_w \leq d_a \\ v_m d_m + v_a (h_w - d_m) + \alpha (h_w - d_a)^m, & d_a \leq h_w \end{cases}$$

$$v_m = k_m i\,,\; v_a = k_a i\,,\; k_m = k_a / \beta\,,\; \alpha = \sqrt{i}\,/\,n \qquad (10)$$

where q is discharge per unit width, h_w is water depth, i is the slope gradient, k_m is the saturated hydraulic conductivity of the capillary soil layer, ka is the hydraulic conductivity of the noncapillary soil layer, dm is the depth of the capillary soil layer, d_a (= h) represents the depths of the capillary and non-capillary soil layers, β is the exponent constant of unsaturated flow, vm and va are the flow velocities of unsaturated and saturated subsurface flows, respectively, and n is the Manning's roughness coefficient varies as a function of land use type.

© 2010 Department of Geological Engineering, Gadjah Mada University

2.3 Critical rainfall

Critical rainfall-induced slope instability for each land unit (grid) inside those areas predefined as potentially "stable/unstable" is predicted by combining those above slope stability model and hydrological approaches. From Eq.(6), the critical saturated soil depth to cause instability is:

$$h_w^c = \frac{h\rho_s}{\rho_w}\left(1 - \frac{\tan\theta}{\tan\phi}\right) + \frac{c_s}{\rho_w g \cos\theta \tan\phi} \quad (11)$$

from stage-discharge relationships (see Eq.10), critical subsurface inflow discharge per unit width into a grid element can be expressed by substituting the critical saturated soil depth into Eq.(12):

$$q^c = \begin{cases} v_m d_m (h_w{}^c / d_m)^\beta, & 0 \le h_w{}^c \le d_m \\ v_m d_m + v_a (h_w{}^c - d_m), & d_m \le h_w{}^c \le d_a \end{cases} \quad (12)$$

Finally, near steady-state critical rainfall rate, rc(mm hr-1), received by each grid can be computed as function of upslope contributing areas, slope length, topographic elements, soil properties, and critical saturated soil depth as follows:

$$r^c(x) = \frac{q^c(x)}{\left(\frac{U}{w} + x\right)} \quad (13)$$

Herein near steady state critical rainfall rate inducing slope instability of a grid element is defined as the total of rainfall rate from the upslope contributing areas and rainfall over the grid.

3 Case study

The Upper Citarum Catchment with Saguling Reservoir as the outlet is located in the mountainous area of West Java Province and lies between 600 to 3000 m. Geographically, the area lies off 107°26′ E-107°95′ E and 6°73′ S-7°25′ S (Figure 3a).

The characteristic of rainfall distribution in the Upper Citarum is not uniform. The climate conditions are characterized by tropical monsoon with two distinct wet and dry seasons. A series of data from BMG specifying that high amount of rainfall is at the beginning of November-December followed by a second peak in March-April as a result of the westerly monsoon. The rainfall amount then quickly slackens down in May-October due to dry season as a result of the prevailing easterly monsoon. Annually, rainfall of the area varies from 1500 mm up to 4000 mm.

The geological formation consists mainly of old quaternary volcanic product with some Miocene sedimentary facies, granite, granodiorite, diorite, alluvium, Pleistocene volcanic facies, and Miocene limestone facies. Due to the influence of the active volcano, the types of soils in the study area varies and are underlined complex. Based on the digitized soil map from Agricultural Department of Indonesia, the andosol-district soil mainly lays on the mountainous area in the northern part that was influenced by volcanic eruption. Black andosol soils can be found in the flat area whereas latosol is stretched along the Lembang fault and alluvial is occupied along sides of the river valley.

4 Model application

4.1 Geotechnical properties of the soil

Six soil samples were returned for laboratory analysis, representing the six principal soil sampling locations. Sampling depth is 80-120 cm, which roughly corresponds to the depth of the potential failure slopes. These were catalogued with a soil type and administrative region. The collected disturbed soil samples were analyzed in the laboratory using a portable direct-shear test apparatus to provide information on soil cohesion and internal slope friction. Direct-shear tests were conducted under three different normal stresses (10, 20, 30, and 40 kPa) for each sample. The test was conducted in the saturated state by filling water into the shear box. The test results (Table 1) were then used to treat slope stability model parameters that was related to geotechnical properties as spatially distributed.

© 2010 Department of Geological Engineering, Gadjah Mada University

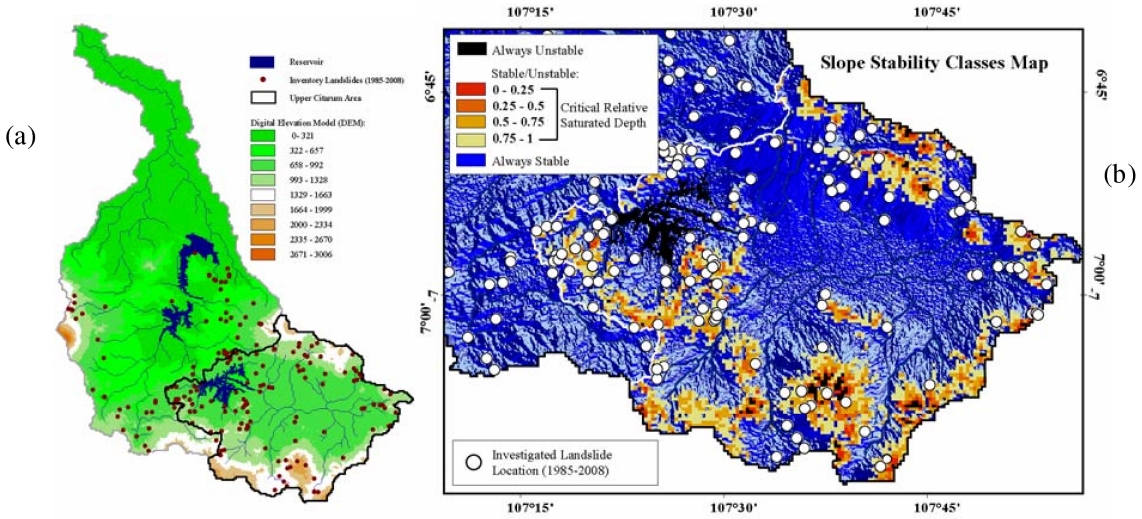

Figure 3: (a) The location of the Upper Citarum River catchment over the whole DEM (90 x 90 m2) Citarum River basin. The red points indicate the locations of landslides as inventoried by the Geological Agency of Indonesia (1985-2008), and (b) Comparison among spatial distribution patterns of estimated time-invariant slope stability classes mapping based on the critical relative saturated depth (mc) and investigated landslide location patterns (1985-2008 as shown by white circles) in the Upper Citarum Catchment

Table 1: Laboratory test results for geotechnical soil properties.

Soil Samples	Soil Cohesion (kPa)	Internal Angle Friction (deg)
Soil Sample 1	7.28	21.62
Soil Sample 2	1.59	5.99
Soil Sample 3	4.49	28.68
Soil Sample 4	10.90	37.89
Soil Sample 5	6.29	17.04
Soil Sample 6	5.69	33.30

4.2 Slope stability classes mapping

A reliable field and laboratory measurement of geotechnical properties (c^s and φ) for the different parent soil materials of the study area was available and slope stability model parameters were estimated on the basis of laboratory test and study literature. Calibration through a comparison of observed landslide locations with model predictions provides an assessment of model reliability. The comparison is obtained by mapping long-term observed landslide (1985-2008) on a map of the predicted time-invariant slope stability classes based on critical relative saturated depth values by grid resolution 90 m (Figure 3b). The figure shows that the patterns of landslide potential area are simulated on the above basis along with the general pattern of observed landslides. The model reproduced several of the principle clusters in the observed pattern.

Two types of error appeared in the spatial pattern of this map: (1) some grids are predicted as theoretically always stable, however landslides were mapped on them, especially at northern part of the study region, and (2) some amount of grids are predicted by model as theoretically always unstable, but no scars were observed on them. Such errors are typically caused by inaccurate topography and soil properties. However, on the basis of these results, the slope stability model by grid resolution of 90 m (http://hydrosheds.cr.usgs.gov) is considered to be utilized effectively for mapping critical rainfall rate and dynamic time-dependent slope stability mapping in response to particular rainfall event in the study site.

© 2010 Department of Geological Engineering, Gadjah Mada University

4.3 Spatial distribution of critical rainfall-induced shallow landslide

Figure 4c shows the distribution of critical rainfall ranges. Lower critical levels (i.e. higher potential for slope failure) principally occupy steep slopes and large contributing areas. In contrast, higher critical rainfall thresholds are present in gentle slopes.

To assess the potential application for shallow landslides prediction and warning, the system was applied to the past new "Cikembang" shallow landslide event (see Figure 4a) and forced by utilizing satellite-derived real-time half-hourly QMORPH rainfall product (http://www.cpc.ncep.noaa.gov/) (Figure 4c). Then the method measures the rainfall intensity difference (RID): the amount of rainfall intensity is above (or below) the critical rainfall. It is assumed that slope failures will more likely occur in areas where (RID) is positive or large. Applied to the past new "Cikembang's" landslide with the critical rainfall rate is estimated approximately 15.03 mm/hr, the model predicts the grid over and nearby to this observed shallow landslides were found in unstable condition in this study several hours before landslides initiation. The time for weighted-area rainfall intensity was more than the critical rainfall rate to occur in the sub-catchment approximated to the time of landslide occurrence as recorded (Figure 4c). A cumulative rainfall depth of 130.0 mm was detected at Cikembang Village on that time (Figure 4b). The total amount of rainfall that triggered these two landslides was characterized as a significant concentration of rainfall and represented "extreme case". The present results have shown a high potential applicability of the proposed method forced by satellite-based rainfall data to detect heavy rain-triggered landslide events in near real-time.

The further study will be intended for establishing rainfall intensity-duration thresholds curve on the basin, catchment, and local scales that is derived based on the previous results and landslide inventory data. In addition, the further study also aims to make the approach more valuable for discerning areas of potential shallow landslide in response to rainfall events and its warning system for whole Indonesian river catchment (Figure 5).

5 Conclusions

This study has presented a novel method that combines deterministic slope stability model and hydrological approach for predicting critical rainfall-induced shallow landslides. Based on the results of model performance, the proposed method is useful for rainfall-triggered shallow landslide disaster warning at large catchment scale. More accurate (quantitatively) and high resolution data, including rainfall, DEM, soil properties, land use, and hydrological-geotechnical observations, are necessary for reasonable landslide predictions.

Acknowledgements

The support from the International Consortium on Landslides (ICL) and Disaster Prevention Research Institute (DPRI), Kyoto University under the projects "Asian Joint Research Project for Early Warning of Landslides" are gratefully acknowledged. The authors would like to thank Jhon E Janowiak (CPC-NOAA), Parwati Sofan (LAPAN, Indonesia) and Sumaryono (the Geological Agency of Indonesia) for their help with satellite-based rainfall information and providing the landslide inventory database.

References

Apip., Sayama, T., Tachikawa, Y., and Takara, K. (2008) Lumping of a physically-based distributed model for sediment runoff prediction in a catchment scale, Annual Journal of Hydraulic Engineering, JSCE, Vol.52, pp 43-48.

Bathurst, J.C., Burton, A., Clarke, B.G., and Gallart, F. (2006) Application of the SHETRAN basin-scale, landslide sediment yield model to the Llobregat basin, Spanish Pyrenees, Hydrological Processes, Vol.20, pp.3119-3138.

Cardinali, M., Galli, M., Guzzetti, F., Ardizzone, F., Reichenbach P., and Bartoccini, P. (2006) Rainfall induced in December 2004 in Southwestern Umbria, Central Italy, Natural Hazards and Earth System Science, Vol.6, pp.237-260.

© 2010 Department of Geological Engineering, Gadjah Mada University

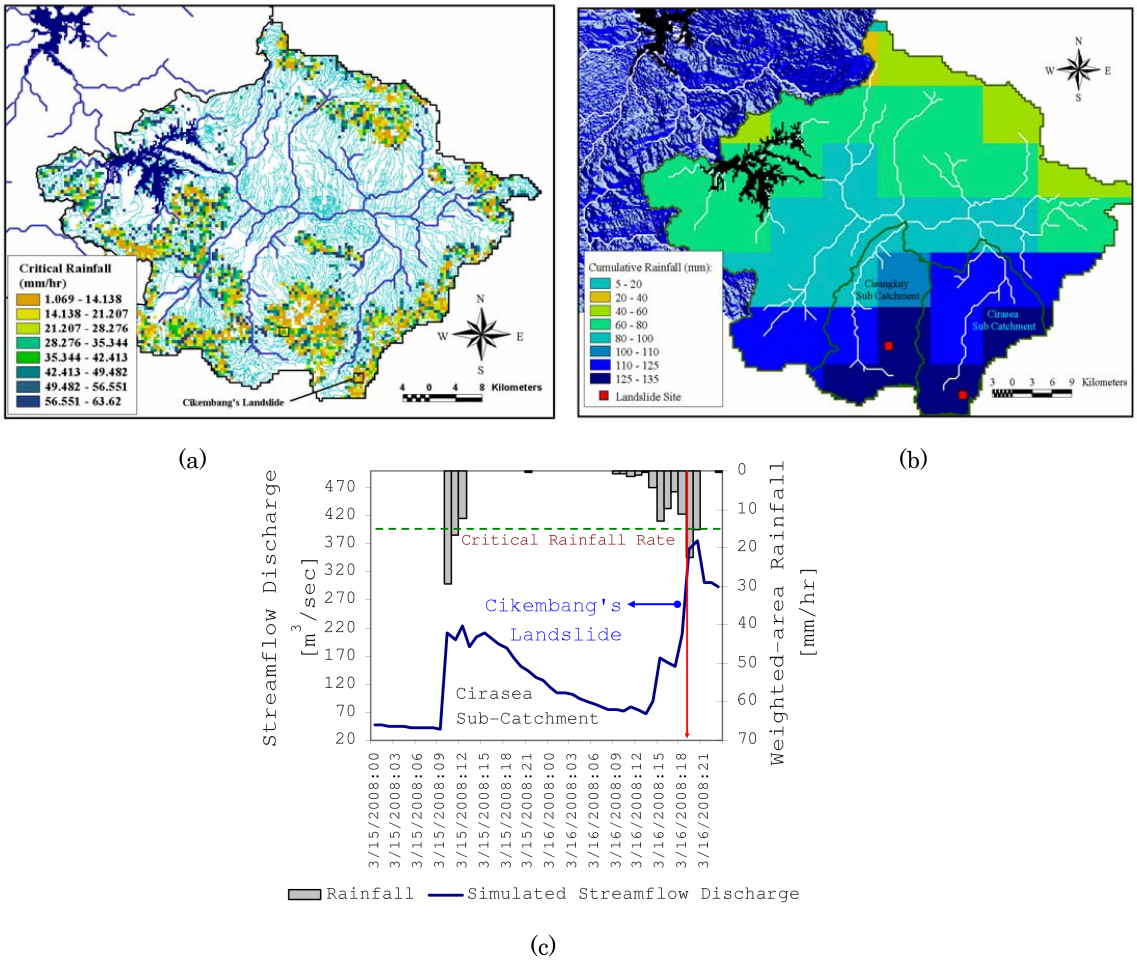

Figure 4: (a) spatial distribution of critical rainfall rate-induced slope instability, (b) cumulative rainfall depth during the rainfall events of 15-16 March 2008 and (c) Weighted-area hyetograph and its simulated river hydrograph at the outlet of sub-catchment where the past "Cikembang" shallow landslides occurred

© 2010 Department of Geological Engineering, Gadjah Mada University

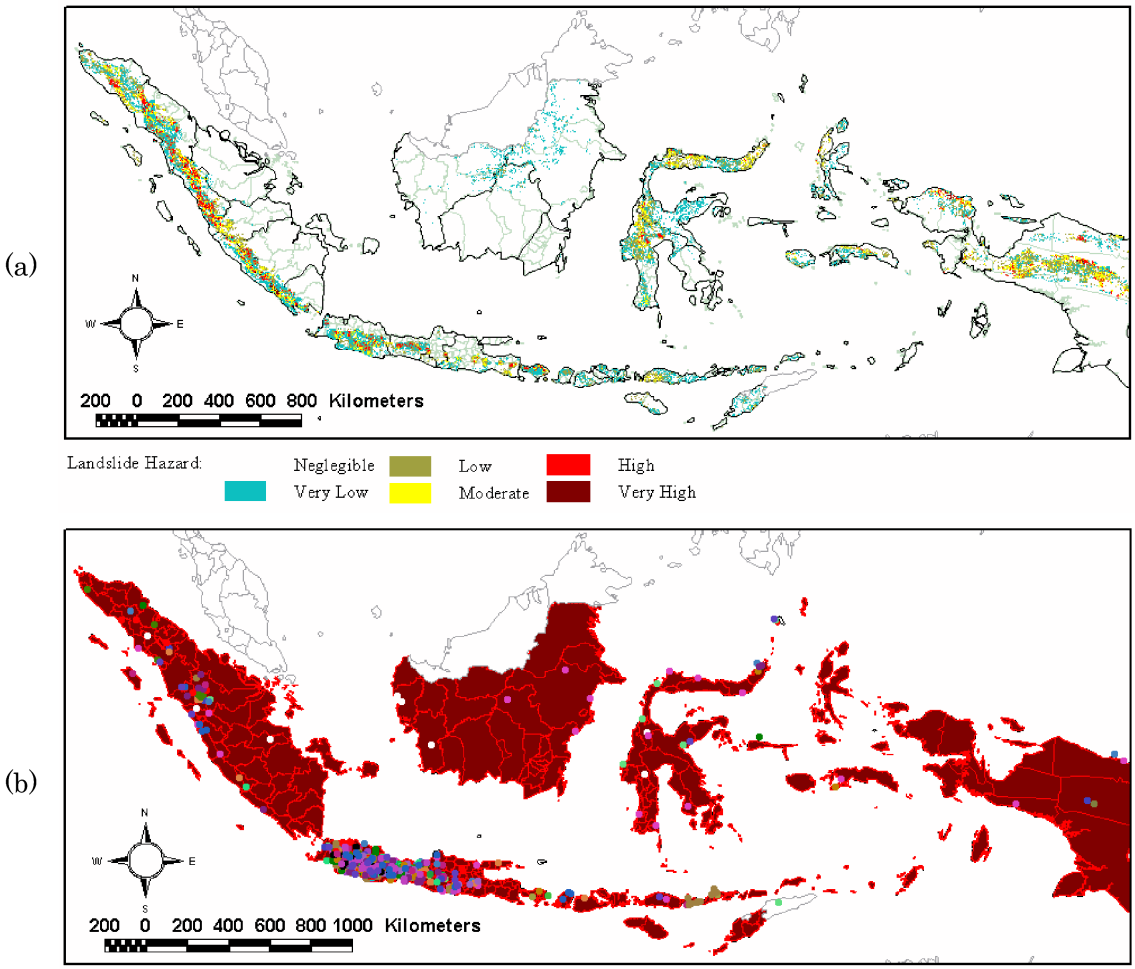

Figure 5: (a) Distribution map of river catchment and landslide inventory (1980-2008) as shown by circles, and (b) Landslide hazard zonation for Indonesia. Data sources: `http://sedac.ciesin.org/gateway/access.html`, `http://portal.vsi.esdm.go.id/joomla/`, and `http://trmm.gsfc.nasa.gov/publications_dir/potential_landslide.html`

© 2010 Department of Geological Engineering, Gadjah Mada University

Chiang, S.H., and Chang, K.S. (2009) Application of radar data to modeling rainfall-induced landslides. Geomorphology, Vol.103, pp.299-309.

Dai, F.C. and Lee, C.F. (2003) A spatiotemporal probabilistic modeling of storm-induced shallow landsliding using aerial photographs and logistic regression, Earth Surface Processes and Landforms, Vol.25, pp.527-545.

Hong, Y., and Adler, R.F. (2008) Predicting global landslide spatio temporal distribution: integrating landslide susceptibility zoning techniques and realtime satellite rainfall estimates, International Journal of Sediment Research, Vol.23, pp. 249257.

Montgomery, D.R., and Dietrich, W.E. (1994) A physically based model for the topographic control on shallow landsliding, Water Resources Research, Vol.30(4), pp.1153-1171.

Tachikawa, Y., Nagatani, G., and Takara, K. (2004) Development of stage-discharge relationship equation incorporating saturated- unsaturated flow mechanism. Annual Journal of Hydraulic Engineering, JSCE, Vol.48, pp.7-12.

 © 2010 Department of Geological Engineering, Gadjah Mada University